Low-temperature quantum relaxation of single two-dimensional vortices in an epitaxial $Tl_2Ba_2Ca_2Cu_3O_x$ thin film

A García, X. X. Zhang, and J. Tejada
Departament de Física Fonamental, Universitat de Barcelona, Diagonal, 647, E-08028, Barcelona, Spain

M. Manzel and H. Bruchlos
Institut für Physikalische Hochtechnologie, Helmholtzweg 4, D-07743 Jena, Germany
(Received 15 February 1994; revised manuscript received 13 June 1994)

Time-logarithmic magnetic-relaxation measurements have been obtained in an epitaxial $Tl_2Ba_2Ca_2Cu_3O_x$ thin film for the zero-field cooled and remanent magnetization, with low and moderate applied magnetic fields. With low fields ($H_a=50$ Oe), the normalized magnetic relaxation rates, $S\equiv|d(M/M_i)/d\ln t|$, are temperature independent below $T\simeq 3.4$ K, and the transition from the thermal to the quantum regime appears to be quite sharp. With moderate fields ($H_a=500$ Oe), the transition becomes smooth and takes place at temperatures higher than with low fields, $T\simeq 7$ K. This seems to indicate that the mechanism responsible for low-temperature relaxation would be nondissipative Hall tunneling of two-dimensional vortices, rather than dissipative vortex motion.

INTRODUCTION

The dynamic magnetic properties of high-T_c superconductors have been widely explored in the last years, particularly through the study of magnetic relaxation of vortices from metastable states. The usual interpretation of this phenomenon known as flux creep has been given in the framework of the classical theory of Anderson,[1] which explains the observed decays of the magnetization as thermally activated vortex motion and predicts normalized relaxation rates vanishing at zero temperature. However, some of the pioneering experiments by Mota *et al.*[2,3] in Sr-La-Cu-O and Ba-La-Cu-O samples with different forms, already showed low-temperature relaxation rates which did not extrapolate to zero at zero temperature; suggesting the existence of some other alternative dissipative mechanism of vortex motion at these temperatures. Further experiments in several Y-Ba-Cu-O samples[4-6] as well as in single-crystal Bi-Sr-Ca-Cu-O (Ref. 7) confirmed the presence of those effects in these materials and suggested different possible explanations,[8-10] among which the tunneling of vortices through pinning energy barriers turned out to be the dominant mechanism in the relaxation process at low temperatures. Very recently, we detected temperature-independent normalized relaxation rates in powdered $Tl_2Ba_2Ca_1Cu_2O_8$ (Ref. 11) and bulk sintered $Tl_2Ba_2Ca_2Cu_3O_{10}$ (Ref. 12) superconductors up to 6.5 and 10 K, respectively, and analyzed them in terms of quantum tunneling of single 2D vortices.[13]

EXPERIMENT

In this paper we present and discuss magnetic relaxation results at low temperatures down to $T=1.8$ K, with low ($H_a=50$ Oe) and moderate ($H_a=500$ Oe) applied magnetic fields, in a superconducting epitaxial $Tl_2Ba_2Ca_2Cu_3O_x$ thin film. A description of the film manufacturing technique has been recently given[14,15] and only the main features are presented here. The epitaxial films of $Tl_2Ba_2Ca_2Cu_3O_x$ (TBCCO) were grown by a two-step method.[16] As a first step, Ba-Ca-Cu-O precursor films were reactively deposited by high-rate dc magnetron sputtering of a metallic $Ba_2Ca_2Cu_3$ alloy target ($\varnothing=100$ mm) onto $LaAlO_3$ substrates up to 50 mm in diameter and 10×10 mm^2 $SrTiO_3$ substrates. Selective resputtering effects can be suppressed at high deposition rates ($R>50$ nm/min), because the desorption rate of the alkaline-earth-metal components was found to be nearly independent of the deposition rate.[14] The as-deposited films on (100)-$LaAlO_3$ and (100)-$SrTiO_3$ substrates are amorphous, isolating, and appear mirror-smooth.

In a second step thallium was incorporated into the precursor films by post-annealing in a Tl-oxide loaded atmosphere for 10 min at 1150 K and subsequent cooling in O_2 with a special computer-controlled temperature program. During this step the sample was enclosed in a gold-platinum container together with a presintered pellet of Tl high-T_c bulk ceramic. Thallium-diffusion experiments with pellets of different compositions (2223, 2222, and 2201) have shown that $Tl_2Ba_2Ca_2Cu_2O_x$ is a useful composition with respect to the durability of the thallium source. Depth profiles, measured by means of secondary neutral mass spectroscopy, indicate that thallium is homogeneously distributed in the annealed thin TBCCO film.[15] However, the annealing of the precursor film is a very critical technology step, in which the film is loaded with thallium, simultaneously crystallized, and fully oxidized.

The superconducting properties of the TBCCO films depend sensitively on the film structure.[17] Therefore, we have investigated the morphology, phase composition, and texture of the films by means of SEM, microprobe

analysis, and x-ray diffraction. A scanning electron micrograph of a TBCCO film is shown in Fig. 1. The coarse-grained films consist of well-connected platelets with diameters of about 80 μm. The crystal structure of our films was investigated by $(\Theta-2\Theta)$, ω, and Φ scan x-ray-diffraction measurements. The TBCCO films consist predominantly of the Tl-(2223) phase with a lattice constant of $c=3.5648$ nm. Furthermore, the post-annealed films are exceptionally well oriented, the half-width of the rocking curve for the (0014) peak being 0.58°. Besides a high c-axis orientation, a nearly perfect in-plane epitaxy of our films was also found. The x-ray-diffraction rotational Φ scan using the $Tl_2Ba_2Ca_2Cu_3O_x$ $(0\bar{4}22)$ reflection is presented in Fig. 2. The peaks (full width at half maximum is 2.05°) at 90° intervals of the Φ scan indicate that the films are epitaxially oriented with respect to the underlying substrate. Furthermore, pole figure measurements demonstrated that the [100] direction of the $Tl_2Ba_2Ca_2Cu_3O_x$ film is aligned with pseudocubic [100] $LaAlO_3$ and [100] $SrTiO_3$. The superconducting properties of 1-μm-thick TBCCO films on $LaAlO_3$ and $SrTiO_3$ substrates are listed in Table I.

RESULTS AND DISCUSSION

Before discussing our results, let us first turn to the discussion on the dimensionality of the object involved in the (quantum as well as thermal) relaxation process. It is known that the usual picture of a flux line as a three-dimensional cylinder traversing a classical type-II superconductor does not apply to high-T_c superconductors due to their layered structure and the tendency of the conductivity to take place only in the CuO_2 planes. Thus, a more adequate picture of a flux line traversing a stack of layers in these materials is a set of nearly circular vortices lying in the copper-oxide layers, the "two-dimensional (2D) pancake vortices," connected by Josephson vortices stretching from the center of one 2D pancake vortex in one layer to the center of another 2D pancake vortex in the next layer. There are several

FIG. 1. SEM micrograph of a $Tl_2Ba_2Ca_2Cu_3O_x$ film prepared on a 25-mm-diam (100) $LaAlO_3$ wafer.

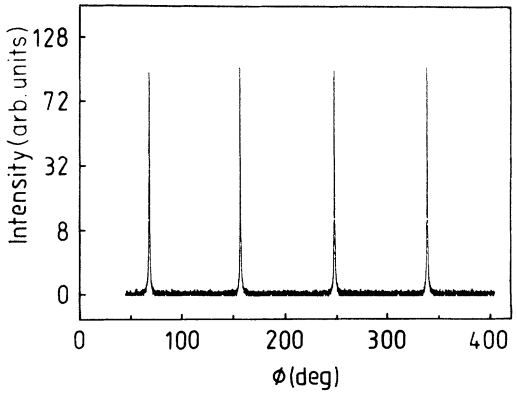

FIG. 2. X-ray-diffraction rotational Φ scan of $Tl_2Ba_2Ca_2Cu_3O_x$ $(0\bar{4}22)$ reflection on $SrTiO_3$ substrate.

reasons which lead us to strongly believe that the objects involved in the relaxation process are nothing but single 2D pancake vortices. First of all, the perpendicular Josephson coupling between two neighboring layers is characterized by a very elliptical current with an associated perpendicular Josephson length[18] $\lambda_\perp=\gamma d$ [where $\gamma=(m_c/m_{ab})^{1/2}$ is the anisotropy constant of the superconductor, and d is the interlayer spacing], in such a way that the larger $\lambda_\perp$, the weaker the Josephson coupling between two neighboring layers. For the Tl-(2223) material, $\gamma\simeq 350$ (Ref. 19) and $d=17.8$ Å,[20] so $\lambda_\perp\simeq 6\times 10^3$ Å $\gg d$. Thus, each copper-oxide layer can be considered independent of adjacent layers. Second, due to the low flux density created in the material by the low and moderate applied magnetic fields, the distance between two 2D pancake vortices in the same layer is large enough to neglect the electromagnetic and Josephson interaction between them and consider each 2D pancake vortex independent of its neighbors. Third, the longitudinal dimension of the relaxing object is given in the quantum-collective creep (QCC) theory for layered superconductors[21] by the collective-pinning length $L_c^c\simeq(\xi/\gamma)(j_0/j_c)^{1/2}$, for magnetic fields applied in the c direction. ξ is the superconducting coherence length, $j_0=(c\Phi_0)/(12\sqrt{3}\pi\lambda^2\xi)$ is the depairing current density, j_c is the critical current density, and λ is the London penetration depth in the **a-b** plane. Using typical values for our superconductor, $(j_0/j_c)^{1/2}\simeq 10$, $\xi\simeq 15$–20 Å, and $\gamma\simeq 350$, we get $L_c^c\simeq 1$ Å $\ll d$, which corresponds to the strong pinning regime where each 2D pancake vortex is pinned individually.[21] Thus, all three arguments ensure that the objects relaxing in the sample are independent, single 2D pancake vortices.

Let us now introduce and discuss our results. All mag-

TABLE I. Superconducting properties of 1-μm-thick thallium films on $LaAlO_3$ and $SrTiO_3$ substrates.

Transition temperature	>110 K, max 118 K
ac susceptibility transition width (90–10%)	<1 K
Critical current density at 77 K	6×10^5 A/cm^2
Surface resistance at 77 K and 25 GHz	(1.4±0.1) mΩ

netic measurements have been performed using a commercial quantum design SQUID magnetometer. Magnetic relaxation was measured with two applied magnetic fields, $H_a = 50$ and 500 Oe, for two different cooling processes. In the first one, known as the zero-field-cooling (ZFC) process, the sample was cooled to a target temperature below T_c in a zero applied magnetic field and, after waiting 500 s for a complete thermal stabilization of the whole sample, a magnetic field was applied perpendicular to the **a-b** plane of the sample. In the second process, known as the field-cooling (fc) process, the sample was cooled down in a nonzero applied field and, after waiting 500 s, the field was switched off. In the former process, the time decay of the zero-field-cooled magnetization ($M_{\rm ZFC}$) was detected, while in the latter the evolution with time of the remanent magnetization ($M_{\rm rem}$) was studied. The total measuring time was 4000 s. Measurements with the magnetic field applied parallel to the **a-b** plane of the sample gave magnetization values 2 orders of magnitude lower than those with the field parallel to the **c** axis, and the relaxation rates were too small to study the dynamic properties with this field configuration.

Figures 3(a) and 3(b) show, respectively, the time evolution of $M_{\rm ZFC}$ and $M_{\rm rem}$, at different temperatures, with $H_a = 50$ Oe. Figures 4(a) and 4(b) show similar data with $H_a = 500$ Oe. All curves show perfect linear logarithmic dependences in the time interval $210 < t < 4000$ s, with a nonlinear transient initial decay during the first 210 s which could correspond to a reconfiguration of the inhomogeneous magnetic flux distribution created by changing the magnetic field.[22] Deviations from that linear behavior were detected at temperatures above 70 K. It should be emphasized that in Figs. 3(a) and 3(b) we observed large decay rates with $H_a = 50$ Oe, comparable to those detected in Figs. 4(a) and 4(b) with $H_a = 500$ Oe. The reason for this is the large demagnetizing factor of a superconducting thin film: $N \simeq 1-(t/w)$,[23] where t and w are the thickness and the width of the sample, respectively. N determines a "real" lower critical field $H_{rc1} = (1-N)H_{c1}$, which is much lower than H_{c1} extracted from the first magnetization curve. For the sample studied here, $t \simeq 1$ μm, $w \simeq 3$ mm, and $H_{c1} \simeq 150$ Oe, so $H_{rc1} \simeq 1$ Oe. Similarly, the field for first full penetration (that is, the field at which the flux first reaches the center of the sample and establishes the critical state) is very much reduced. Thus, $H_a = 50$ Oe is large enough to establish the critical state within the material, and large relaxation rates can be detected.

Figures 5(a) and 5(b) show the temperature dependence of the magnetic viscosity, $S \equiv |d(M/M_i)/d\ln t|$. These rates were obtained from the linear fitting of the relaxation data to a time-logarithmic law in the time interval $210 < t < 4000$ s. A magnification of the low-temperature regime ($T/T_c \leq 0.15$) is shown in Figs. 6(a) and 6(b). Notice that the magnetic viscosities corresponding to $M_{\rm ZFC}$

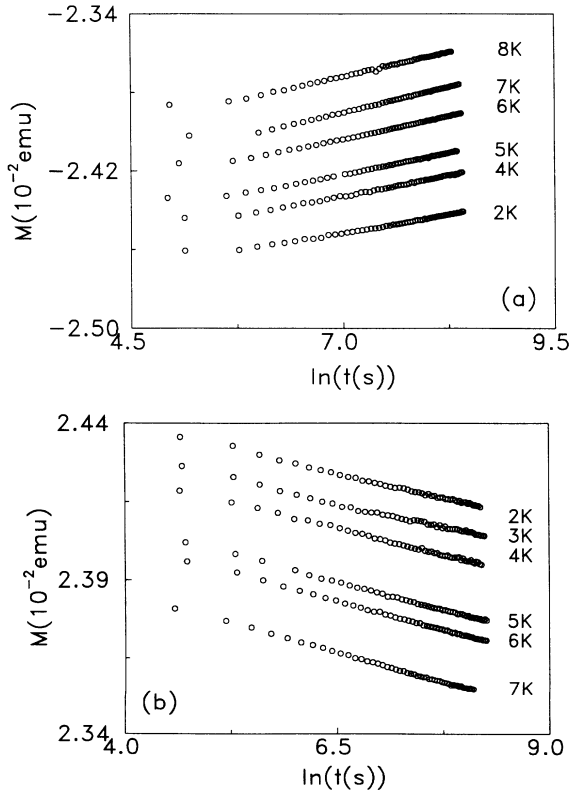

FIG. 3. Time-logarithmic magnetic relaxation curves at different temperatures with $H_a = 50$ Oe: (a) $M_{\rm ZFC}$ vs $\ln[t(s)]$, and (b) $M_{\rm rem}$ vs $\ln[t(s)]$.

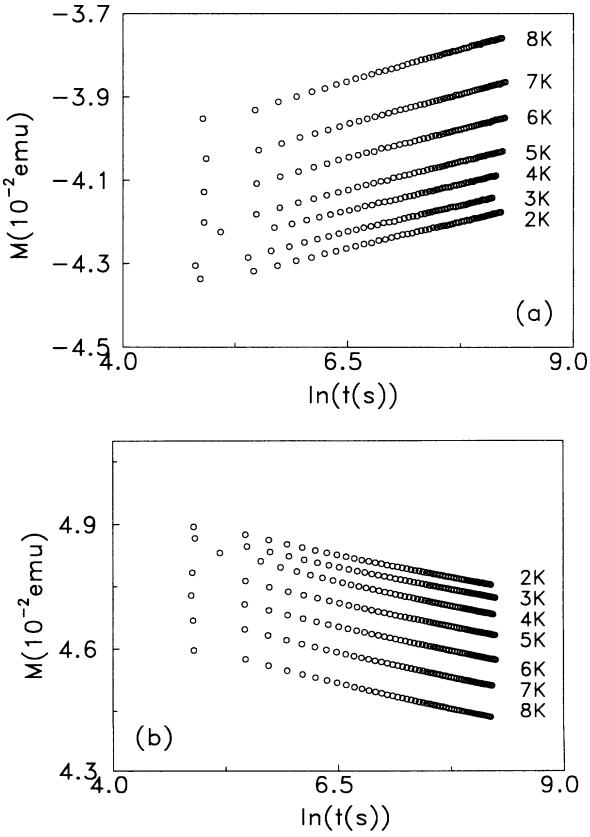

FIG. 4. Low-temperature time-logarithmic magnetic relaxation data with $H_a = 500$ Oe: (a) $M_{\rm ZFC}$ vs $\ln[t(s)]$, and (b) $M_{\rm rem}$ vs $\ln[t(s)]$.

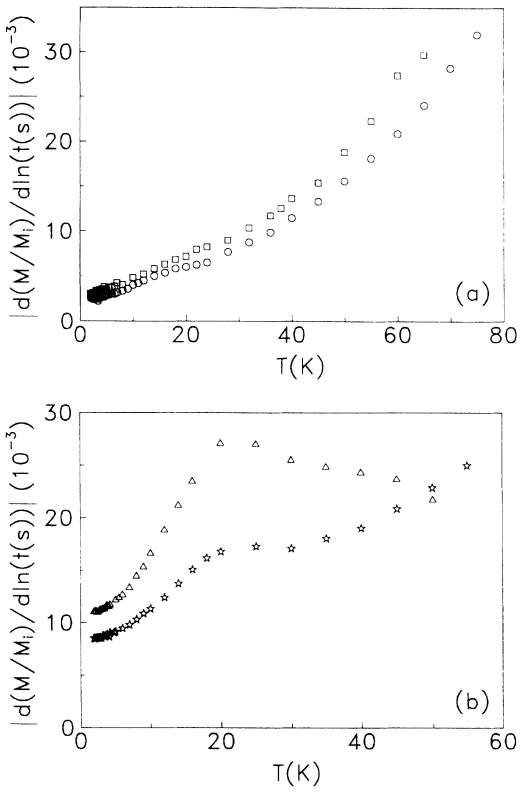

FIG. 5. Temperature dependence of the magnetic viscosity. In (a) ($H_a=50$ Oe), the squares correspond to $M_{\rm ZFC}$ and the circles to $M_{\rm rem}$; in (b) ($H_a=500$ Oe), the triangles correspond to $M_{\rm ZFC}$ and the stars to $M_{\rm rem}$.

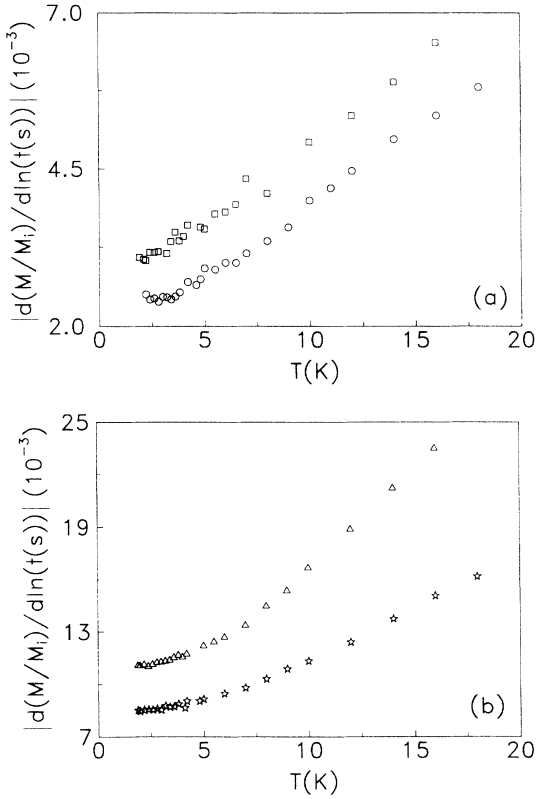

FIG. 6. (a) and (b) show a magnification of the low-temperature regime of Figs. 5(a) and 5(b), respectively. The symbols are the same as in that figure.

and $M_{\rm rem}$ in a given magnetic field are very similar but not equal, indicating the presence of self-field effects which are important in modifying the field profiles at low fields. A common feature of all four curves, which is the first main result of our work, is the change of the magnetic viscosity from a linear dependence to a temperature-independent value, as the temperature decreases below a certain temperature $T_{\rm cr}$. This change is the experimental evidence of a crossover in the mechanism dominating the relaxation process, from the thermally activated vortex motion over pinning energy barriers to the quantum escape of vortices from metastable states under the barriers.[24] This transition appears to be quite sharp in Fig. 6(a). Thus, the crossover temperature may be accurately determined at the point where the sharp transition occurs. This gives $T_{\rm cr,gra}\simeq 3.2$ and 3.6 K for the ZFC and FC magnetic viscosity curves in $H_a=50$ Oe, respectively. On the contrary, the transition in Fig. 6(b) it is seen to be smooth, so the crossover temperature should be determined at the intersection of the temperature-independent plateau and the extrapolation of the linear T dependence down to lower temperatures. The resulting value is $T_{\rm cr,gra}\simeq 5$ K for both the ZFC and FC curves in $H_a=500$ Oe.

The crossover temperature can be first estimated by just equating, at $T_{\rm cr}$, the quantum relaxation frequency, $\Gamma_Q\sim\nu\exp(-B)$, to the thermal relaxation frequency, $\Gamma_T\sim\nu\exp(-U/k_BT)$. Here ν is the attempt frequency, on the order of 10^9–10^{11} Hz; B is the WKB exponent at zero temperature, which can be determined as $1/S(T\rightarrow 0)$; and U is the pinning energy barrier, which can be obtained from the slope of the linear dependence of the magnetic viscosity because, in principle, $S(T)=k_BT/U$ in this regime.[1] This gives $T_{\rm cr,est1}\simeq 12.5$ and 10.5 K for the ZFC and FC curves in Figs. 6(a), and $T_{\rm cr,est1}\simeq 9.5$ and 14.5 K for the ZFC and FC curves in Fig. 6(b), respectively. The large disagreement found between the graphically determined and the estimated values comes from the fact that the linear dependence does not extrapolate to zero as $T\rightarrow 0$, but intersects the S axis in a non-negligible value which must be considered as an additional term to $S(T)$ when determining the energy barrier U: $S(T)=k_BT/U+S(0)$. When taking this term into account, the resulting crossover temperatures are $T_{\rm cr,est2}\simeq 2.9$ and 3.6 K for the ZFC and FC curves at 50 Oe, respectively, in close agreement with those graphically derived. A more physical interpretation lies in the fact that the correct expression for $S(T)$ in the linear regime is $S(T)=k_BT/\langle U\rangle$, where $\langle U\rangle$ is the average energy barrier taken over the energy barrier distribution, and in principle $\langle U\rangle\neq U$ ($\langle U\rangle=U$ only for a single energy barrier). The accurate estimation of $T_{\rm cr}$ for $H_a=500$ Oe will be given below. Table II summarizes the previously experimental and estimated crossover temperatures.

Let us now turn to the discussion on the magnetic viscosity and crossover temperature with $H_a=500$ Oe.

TABLE II. Experimental and estimated crossover temperatures for the ZFC and FC processes with $H_a = 50$ and 500 Oe. $T_{cr,gra}$ has been graphically determined, $T_{cr,est1}$ has been estimated equating the thermal rate to the quantum rate, and $T_{cr,est2}$ has been estimated from the analytical intersection of the fittings of the thermal and quantum regimes.

H_a (Oe)	Cooling process	$T_{cr,gra}$ (K)	$T_{cr,est1}$ (K)	$T_{cr,est2}$ (K)
50	ZFC	3.2	12.6	2.9
50	FC	3.6	10.5	3.6
500	ZFC	5	9.6	7.3
500	FC	5	14.4	8.2

The gradual transition obtained when the magnetic field increases has been usually ascribed to the influence of dissipation on quantum relaxation: It is theoretically predicted[25] and calculated[26] that the quantum decay rate changes gradually with temperature from classical hopping into quantum tunneling, giving rise to a large transition region in which thermally assisted quantum tunneling occurs. Thus, in principle, the magnetic viscosity pattern found with $H_a = 500$ Oe would suggest the presence of dissipation. Nevertheless, it is a remarkable result that the crossover temperatures graphically derived with $H_a = 500$ Oe are higher than those obtained with $H_a = 50$ Oe, in disagreement with the prediction that dissipation lowers T_{cr}.[27] Very recently, Feigel'man *et al.*[28] suggested that it is likely that HSTC may belong to a class of "very clean" type-II superconductors, in which there should be no dissipation at low temperatures. In this limit, the quantum tunneling of vortices is governed by the Hall term in the equation of motion, and the quantum exponent in the two-dimensional case is given by $S^{\text{eff}}/\hbar \sim n_s^{(2)} \xi^2$, where S^{eff} is the Euclidean action, and $n_s^{(2)}$ is the superconducting density per layer. An estimation of this exponent gives an order of magnitude of $\sim 10^2$,[28] in agreement with the magnetic viscosity experimentally found with $H_a = 500$ Oe.[29] On the other hand, in the nondissipative limit, the low-temperature corrections to the quantum rate are proportional to $\exp(-T_0/T)$. The experimental data in the transition region were fitted with great accuracy to the law $S = S_0 + a \exp(-T_0/T)$, and the following parameters were obtained:

$$S = 11.1 + 11.7 \exp(-11.7/T) \text{ for the ZFC curve up to 6–7 K ,}$$

$$S = 8.5 + 7.4 \exp(-12.2/T) \text{ for the FC curve up to 7–8 K .}$$

Above this temperature, the data follow a linear dependence on T. The intersection of the two dependences will give the analytical crossover temperature. This gives $T_{cr} \simeq 7$ and 7.5 K for the ZFC and FC curves, respectively, in close agreement with the upper fitting limits mentioned above. The accurate fittings and the close agreement found in the crossover temperatures strongly support the interpretation in terms of Hall tunneling of 2D vortices in the Cu-O layers.

CONCLUSIONS

In summary, we have detected magnetic relaxation measurements in superconducting $Tl_2Ba_2Ca_2Cu_3O_x$ epitaxial thin film, and interpreted them in terms of single 2D pancake vortex motion. Quantum tunneling manifests itself at low temperatures. The crossover temperature and the shape of the transition from the thermal to the quantum regime change with the applied magnetic field. In particular, T_{cr} is seen to increase when the magnetic field is increased. An interpretation in terms of Hall tunneling of 2D vortices is given. This is, to date, the first experimental detection of low-temperature quantum effects in superconducting thallium thin films.

ACKNOWLEDGMENTS

A. García thanks the Commissionat per a Universitats i Recerca del Departament de la Presidència de la Generalitat de Catalunya for the research grant. X. X. Zhang acknowledges financial support from the CIRIT (Comissió Interdepartamental de Recerca i Innovació Tecnològica) de la Generalitat de Catalunya. J. Tejada thanks the Fundación Domingo Martínez.

[1] P. W. Anderson, Phys. Rev. Lett. **9**, 309 (1962).
[2] A. C. Mota, A. Pollini, P. Visani, K. A. Müller, and J. G. Bednorz, Phys. Rev. B **36**, 4011 (1987); Phys. Scr. **37**, 823 (1988); Physica C **153-155**, 67 (1988).
[3] A. C. Mota, A. Pollini, G. Juri, P. Visani, and B. Hilti, Physica A **168**, 298 (1990).
[4] A. Hamzic, L. Fruchter, and I. A. Campbell, Nature **345**, 515 (1990).
[5] A. C. Mota, G. Juri, P. Visani, A. Pollini, T. Teruzzi, K. Aupke, and B. Hilti, Phsyica C **185-189**, 343 (1991).
[6] L. Fruchter, A. P. Malozemoff, I. A. Campbell, J. Sanchez, M. Konczykowski, R. Griessen, and F. Holtzberg, Phys. Rev. B **43**, 8709 (1991).
[7] D. Prost, L. Fruchter, I. A. Campbell, N. Motohira, and M. Konczykowski, Phys. Rev. B **47**, 3457 (1993).
[8] A. V. Mitin, Zh. Eksp. Teor. Fiz. **93**, 590 (1987) [Sov. Phys. JETP **66**, 335 (1993)].
[9] E. Simánek, Phys. Lett. A **139**, 183 (1989).
[10] J. Z. Sun, C. B. Eom, B. Lairson, J. C. Bravman, and T. H. Geballe, Phys. Rev. B **43**, 3002 (1991).
[11] A. García, X. X. Zhang, A. M. Testa, D. Fiorani, and J. Tejada, J. Phys. Condens. Matter **4**, 10 341 (1992).

[12]X. X. Zhang, A. García, J. Tejada, Y. Xin, and K. W. Wong (unpublished).
[13]J. Tejada, E. M. Chudnovsky, and A. García, Phys. Rev. B **47**, 11 552 (1993).
[14]M. Manzel, H. Bruchlos, E. Steinbeiβ, T. Eick, M. Klinger, J. Fuchs, and B. Kley, Physica C **201**, 337 (1992).
[15]M. Manzel, H. Bruchlos, G. Bruchlos, T. Eick, E. Steinbeiβ, and J. Taubert (unpublished).
[16]C. Y. Qui and I. Shih, Appl. Phys. Lett. **53**, 1122 (1988).
[17]W. L. Holstein, L. A. Parisi, C. Wilker, and R. B. Flippen, IEEE Trans. Appl. Supercond. **3**, 1197 (1993).
[18]J. R. Clem, Phys. Rev. B **43**, 7837 (1991).
[19]D. E. Farrell, R. G. Beck, M. F. Booth, C. J. Allen, E. D. Bukowski, and D. M. Ginsberg, Phys. Rev. B **42**, 6758 (1990).
[20]R. M. Hazen, L. W. Finger, R. J. Angel, C. T. Prewitt, N. L. Ross, C. G. Hadidiacos, P. J. Heaney, D. R. Veblen, Z. Z. Sheng, A. El Ali, and A. M. Hermann, Phys. Rev. Lett. **60**, 1657 (1988).
[21]G. Blatter and V. Geshkenbein, Phys. Rev. B **47**, 2725 (1993).
[22]C. Rossel and P. Chaudhari, Physica C **153-155**, 306 (1988).
[23]A. C. Rose-Innes and E. H. Rhoderick, *Introduction to Superconductivity,* 2nd ed. (Pergamon, New York, 1986), p. 105.
[24]A. J. Leggett, J. Phys. (Paris), Colloq. **39**, C6-1264 (1978).
[25]A. O. Caldeira and A. J. Legget, Phys. Rev. Lett. **46**, 211 (1981).
[26]H. Grabert, P. Olschowski, and U. Weiss, Phys. Rev. B **32**, 3348 (1985).
[27]H. Grabert and U. Weiss, Phys. Rev. Lett. **53**, 1787 (1984).
[28]M. V. Feigel'man, V. B. Geshkenbein, A. I. Larkin, and S. Levit, Pis'ma Zh. Eksp. Teor. Fiz. **57**, 699 (1993) [Sov. Phys. JETP Lett. **57**, 711 (1993)].
[29]Notice that S used to refer to the magnetic viscosity is just $-\hbar/S^{\text{eff}}$.

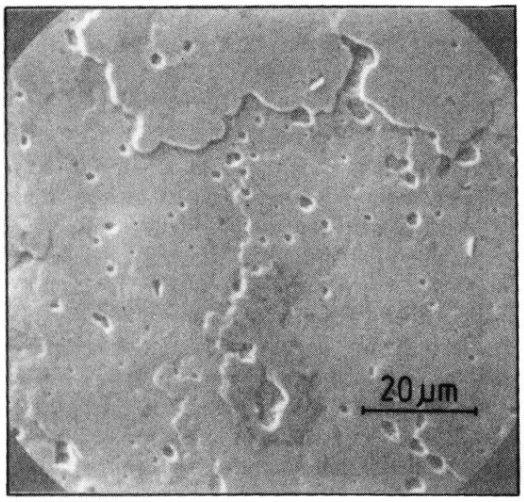

FIG. 1. SEM micrograph of a $Tl_2Ba_2Ca_2Cu_3O_x$ film prepared on a 25-mm-diam (100) $LaAlO_3$ wafer.